Science Bulletin 62 (2017) 1433–1438

Contents lists available at ScienceDirect

Science Bulletin

journal homepage: www.elsevier.com/locate/scib

Article

Optical observations of LIGO source GW 170817 by the Antarctic Survey Telescopes at Dome A, Antarctica

Lei Hu [a,b,c], Xuefeng Wu [a,b,c], Igor Andreoni [d,e,f], Michael C. B. Ashley [g], Jeff Cooke [d,e,h], Xiangqun Cui [i,b], Fujia Du [i], Zigao Dai [j], Bozhong Gu [i], Yi Hu [k,b], Haiping Lu [i], Xiaoyan Li [i], Zhengyang Li [i], Ensi Liang [j], Liangduan Liu [j], Bin Ma [k,b], Zhaohui Shang [l,k,b], Tianrui Sun [a,b,m], N. B. Suntzeff [n], Charling Tao [o,p], Syed A. Uddin [a,b,h], Lifan Wang [n,a,b,*], Xiaofeng Wang [p], Haikun Wen [i], Di Xiao [j], Jin Xu [i], Ji Yang [a], Shihai Yang [i], Xiangyan Yuan [i,b], Hongyan Zhou [q], Hui Zhang [j], Jilin Zhou [j], Zonghong Zhu [r,s]

[a] *Purple Mountain Observatory, Chinese Academy of Sciences, Nanjing 210008, China*
[b] *Chinese Center for Antarctic Astronomy, Nanjing 210008, China*
[c] *School of Astronomy and Space Sciences, University of Science and Technology of China, Hefei 230029, China*
[d] *Centre for Astrophysics and Supercomputing, Swinburne University of Technology, Hawthorn, VIC 3122, Australia*
[e] *The Australian Research Council Centre of Excellence for Gravitational Wave Discovery (OzGrav), Australia*
[f] *Australian Astronomical Observatory, North Ryde, NSW 2113, Australia*
[g] *School of Physics, University of New South Wales, NSW 2052, Australia*
[h] *The Australian Research Council Centre of Excellence for All-Sky Astrophysics (CAASTRO), Australia*
[i] *Nanjing Institute of Astronomical Optics and Technology, Nanjing 210042, China*
[j] *School of Astronomy and Space Science and Key Laboratory of Modern Astronomy and Astrophysics in Ministry of Education, Nanjing University, Nanjing 210093, China*
[k] *National Astronomical Observatories, Chinese Academy of Sciences, Beijing 100012, China*
[l] *Department of Physics, Tianjin Normal University, Tianjin 300074, China*
[m] *Shanghai Key Laboratory for Astrophysics, Shanghai Normal University, Shanghai 200234, China*
[n] *George P. and Cynthia Woods Mitchell Institute for Fundamental Physics & Astronomy, Texas A. & M. University, Department of Physics and Astronomy, 4242 TAMU, College Station, TX 77843, USA*
[o] *Aix Marseille Univ, CNRS/IN2P3, CPPM, Marseille, France*
[p] *Physics Department and Tsinghua Center for Astrophysics (THCA), Tsinghua University, Beijing 100084, China*
[q] *Polar Research Institute of China, Shanghai 200136, China*
[r] *Department of Astronomy, Beijing Normal University, Beijing 100875, China*
[s] *School of Physics and Technology, Wuhan University, Wuhan 430072, China*

ARTICLE INFO

Article history:
Received 12 October 2017
Received in revised form 13 October 2017
Accepted 13 October 2017
Available online 16 October 2017

Keywords:
Gravitational waves
Binary neutron stars
Gamma-ray bursts

ABSTRACT

The LIGO detection of gravitational waves (GW) from merging black holes in 2015 marked the beginning of a new era in observational astronomy. The detection of an electromagnetic signal from a GW source is the critical next step to explore in detail the physics involved. The Antarctic Survey Telescopes (AST3), located at Dome A, Antarctica, is uniquely situated for rapid response time-domain astronomy with its continuous night-time coverage during the austral winter. We report optical observations of the GW source (GW 170817) in the nearby galaxy NGC 4993 using AST3. The data show a rapidly fading transient at around 1 day after the GW trigger, with the *i*-band magnitude declining from 17.23 ± 0.13 magnitude to 17.72 ± 0.09 magnitude in ~ 1.8 h. The brightness and time evolution of the optical transient associated with GW 170817 are broadly consistent with the predictions of models involving merging binary neutron stars. We infer from our data that the merging process ejected about $\sim 10^{-2}$ solar mass of radioactive material at a speed of up to 30% the speed of light.

1. Introduction

On August 17, 2017, the LIGO-Virgo gravitational wave (GW) detector network observed a GW signal from a binary neutron star (BNS) merger, referred to as GW 170817 [1–6]. A short gamma ray

* Corresponding author.
E-mail address: lifanwang@gmail.com (L. Wang).

https://doi.org/10.1016/j.scib.2017.10.006
2095-9273/

burst (SGRB), GRB 170817A, was detected by the GBM instrument on board NASA's *Fermi* satellite less than 2 s after the GW detection [7]. The object was also observed by ESA's *INTEGRAL* satellite [8]. The association of a γ-ray burst with GW 170817A triggered a massive number of follow-up observations by ground-based telescopes which very quickly led to the identification of the optical counterpart of GW 170817 in a nearby galaxy NGC 4993. This intensive campaign provides strong evidence for the BNS merger scenario of GW 170817 and marks the beginning of a new era of multi-messenger astronomy.

Following the announcement of GW 170817 and GRB 170817A, the optical counterpart known as AT2017gfo was discovered by the One-Meter, Two Hemisphere (1M2H) team using the 1-m Swope telescope. The object was found to be located in the galaxy NGC 4993, and the first detection was carried out less than 11 h after the detection of GW 170817 [9]. Many other teams also made independent discoveries and observations of this target [10].

BNS mergers produce rapidly evolving optical and infrared transients accompanied by the radiation of gravitational waves [11–15]. Radioactive materials synthesized in the rapid neutron capture process (r-process) are ejected during the merger. The decay of these radioactive materials results in optical and infrared emission with a typical duration of a day to a week [16–23], and a peak luminosity that is about a few thousand times that of a typical nova. Such transient objects in the optical are given the name kilonovae (or macronovae). In contrast to binary black hole mergers, where there is no consensus on the detectability of electromagnetic radiation after the merger, kilonovae are expected to be detectable in both GW and optical/IR bands at a distance up to a few 10 Mpc. Before GW 170817, several kilonovae candidates were identified during follow-up observations of SGRBs, including GRB 130603B [24,25], GRB 050709 [26], GRB 060614 [27], and GRB 080503 [28,29]. Simultaneous detection of a kilonova and a SGRB associated with a GW event would provide key clues to the properties of the ejecta of BNS mergers.

In this paper, we present follow up observations of GW 170817 and its electromagnetic counterpart AT2017gfo by AST3-2, the second telescope of the Antarctic Survey Telescopes at Dome A, Antarctica. In Section 2, we present the instrument, observations, and data reduction in detail. In Section 3, we apply an analytic kilonova model to the temporal evolution of the optical transient associated with GW 170817 acquired by AST3-2 to constrain the most fundamental physical properties related to GW 170817. Our data establishes that optical signals from GW 170817 are consistent with kilonova models. We summarize our results in Section 4.

2. Instrument, observations and data reduction

The AST3-2 is a catadioptric optical telescope with an entrance pupil diameter of 500 mm and an *f*-ratio of 3.73. The telescope is located at Dome A, Antarctica [30,31]. Its unique location allows for continuous observations lasting longer than 24 h during the austral winter. The continuous time coverage is important for many applications of time-domain astronomy (e.g., [32–34]. It is equipped with a 10 K $\times$ 10 K CCD camera in frame transfer mode that provides a field of view of 4.14 deg^2 [35]. The AST3 camera has 16 amplifiers with half of the area masked for frame transfer charge storage. The camera does not need a mechanical shutter to operate. The entire observatory is controlled remotely using the Iridium satellite system to transmit operational commands. Dome A is a site with the lowest temperature and the lowest absolute humidity on earth [34,36–38]. The weather conditions are suitable for taking data for over 95% of the time during the winter. We achieved a full year of remotely controlled operation for the first time during the austral winter in 2017.

The optical counterpart AT2017gfo is located at the coordinates RA = 13:09:48.089 and DEC = –23:22:53.35, about 2.2 kpc from the center of the host galaxy NGC 4993 [9]. AST3-2 observed this target from August 18 through August 28 in *i*-band [39]. The coordinates of the target are not ideal for AST3-2, which is located at a latitude of $-80^\circ\ 22'$. At the time of observations, the maximum elevation of the Sun was already too high to allow for multi-day continuous observations. Nevertheless, a total of 262 exposures were obtained, with each having an exposure time of 300 s except for the first 5 images with exposure times of 60 s. The gap between the exposures is typically 54 s. Due to the low altitude of the target and the rising Sun, the target was only observable for about 2 h each day. Data reported in this paper consist of a total of 91 images taken during the period from Aug. 18, 2017 to Aug. 23, 2017. Data taken after Aug. 24, 2017 show no detectable transients at the position of GW 170817 and will not be discussed in this paper. Data adjacent in time are stacked to produce the final light curves, the dates of observations are shown in Table 1.

Data reduction follows the standard procedure of bias and overscan subtraction, and flat-field correction. Cosmic rays were removed with a Laplacian Edge Detection algorithm, which is a reliable method for identifying and removing cosmic rays [40]. Special treatment was applied to the removal of the structures produced by saturated stars that spread to all the 16 readout channels through cross-talks among the channels. It is possible to construct a very accurate correction of the effect of cross-talk. The pixels affected by cross-talks follow a well defined pattern. The strength of the cross-talk is a function of the pixel values of the (near) saturated pixels [41] of the stars causing the cross-talk. Fig. 1 shows an image affected by amplifier cross-talk and the same image after correction.

The relatively bright host galaxy makes direct aperture photometry difficult. Difference images using late time observations as a template were needed to be constructed for reliable photometry. This required precise astrometric registration of the images. After the preliminary overscan and flat-field corrections, all sky background subtracted images were re-aligned by matching the coordinates of field stars in all images to their corresponding coordinates in the reference frame. The reference frame was constructed using an image taken on Aug. 23, 2017 in the best seeing conditions. During the matching process, we employed a Lanczos-3 interpolation kernel proposed by [42]. The weight of each registered image during the co-adding process was derived from the equation recommended by Ref. [43], which was successfully applied to the co-adding of SDSS Stripe 82 images,

$$w = \frac{F}{\mathrm{FWHM}^2\ V}, \qquad (1)$$

where *F* is characterized by the flux-based photometric zero point, and *V* is the variance of background noise. Such a weighting scheme gives larger weights to images with good seeing conditions and low background levels.

On Aug 23, 2017, the optical transient had faded significantly. This allowed us to use the co-added image of Aug 23, 2017 as the template for subtraction without introducing serious errors in photometric measurements of earlier data. We employed a bivariate polynomial differential background map and a spatially varying PSF for the image subtraction [44]. Images of all other epochs were convolved/deconvolved with spatially varying PSFs to match the resolution and flux scale of the template image. The background and the shape of the PSF were solved simultaneously in Fourier space to minimize the difference between the images. After these steps, the GW optical counterpart is recovered nicely in the difference image (Fig. 2).

Table 1
AST3-2 Photometric Data of the Kilonovae Associated with GW170817

IMAGE ID	UT obs start	UT obs end	UT obs average	m_i (mag)	Δm_i (mag)	$3\ \sigma\ m_{i,\text{limit}}$ (mag)	Caveat
0818a	2017 08 18.54773909	2017 08 18.55200144	2017 08 18.54987027	17.23	0.13	18.25	...
0818b	2017 08 18.58207886	2017 08 18.60667793	2017 08 18.59437840	17.61	0.07	19.47	...
0818c	2017 08 18.60671538	2017 08 18.64366066	2017 08 18.62518802	17.72	0.09	19.53	...
0820	2017 08 20.59673272	2017 08 20.74696424	2017 08 20.67184848	18.67	...	18.67	Upper limit
0821	2017 08 21.54887044	2017 08 21.75227890	2017 08 21.65057467	18.38	...	18.38	Upper limit
0823	2017 08 23.55072740	2017 08 23.62820195	2017 08 23.58946468	...	...	19.64	Template image

Left to right columns are:
(1) coadd image ID,
(2) start time of observation for coadded image,
(3) end time of observation for coadded image,
(4) average time of the observation,
(5) *i*-band magnitude,
(6) photometric error of *i*-band magnitude,
(7) 3σ limiting magnitude of the coadded image, and.
(8) caveat on the coadded image.

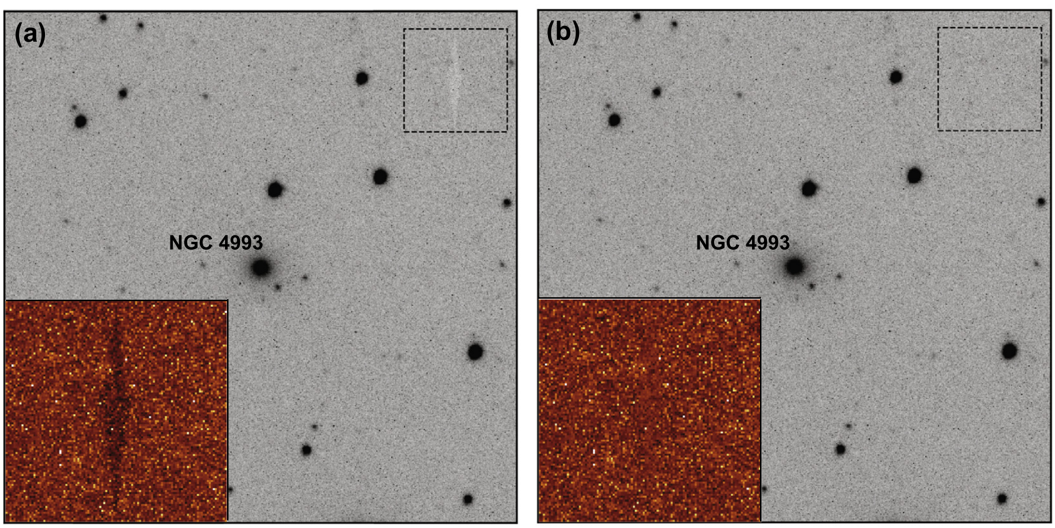

Fig. 1. (Color online) The Correction of CCD Amplifier Cross-Talk. (a) Raw image with cross-talk contamination uncorrected. A dashed square in the upper right corner marks the position of a typical cross-talk affected region. The details of the region is shown in the insert at the lower left corner. (b) Same as (a), but with the cross-talk affected region corrected.

The AAVSO Photometric All-Sky Survey (APASS, [45]) was employed as the catalog for absolute flux calibration. Bright stars around NGC 4993 were selected and the optimal photometry aperture was determined using

$$d = 2 \times 0.6731 \times \text{FWHM}_0, \tag{2}$$

where d is the diameter of the aperture and FWHM_0 is the mean full-width at half-maximum of the standard stars around the target [46]. All photometric results are listed in Table 1. As shown in Fig. 2, the optical signals associated with GW 170817 were detected at $\alpha(J2000.0) = 13^h09^m48^s.082, \delta(J2000.0) = -23^\circ22'53''.60$ on the co-added images of Aug. 18, 2017, while no detectable signal was recovered at this coordinate on Aug. 20, 2017 and Aug. 21, 2017, leading only to photometric upper limits.

3. Theoretical interpretation

As can be seen in Table 1 and Fig. 3, the optical transient in *i*-band faded rapidly with a change of $\Delta m \sim 0.5$ in $\Delta t \sim 1.8$ h at $t \sim 1$ day after the detection of GW 170817. Such fast intra-day evolution of the light curve is consistent with the predictions of kilonova models, as also suggested by a broad range of other independent electromagnetic observations using many different telescopes by the LIGO/Virgo scientific collaboration [10].

A general approach in determining the properties of a kilonova is to model the observed data with a detailed radiative transfer simulation [18–22]. However, a simple analytic model is sufficient for deriving the basic physical parameters of the kilonova. In the following, we will use a simplified kilonova model to fit the data points obtained by AST3-2.

We model the bolometric light curve of the kilonova using the formula [47–49]

$$L_{\text{MN}} = M_{\text{ej}}\epsilon_{\text{th}}\,\dot{\epsilon}_0 \times \begin{cases} \frac{t}{t_c}\left(\frac{t}{1\ \text{day}}\right)^{-1.3}, & \text{if } t \leqslant t_c, \\ \left(\frac{t}{1\ \text{day}}\right)^{-1.3}, & \text{if } t > t_c, \end{cases} \tag{3}$$

here we adopt $\dot{\epsilon}_0 = 1.58 \times 10^{10} \text{erg g}^{-1}\,\text{s}^{-1}$ and the thermalization efficiency $\epsilon_{\text{th}} = 0.5$ following [48]. t_c is the critical time, after which $(t > t_c)$ the ejecta becomes transparent. [47,48] found that the bolometric light curve of this analytic model function can reasonably match the results of the radiation-transfer simulation performed in Ref. [21].

The spectrum of the kilonova emission is determined by complex frequency-dependent radiative processes within its ejecta.

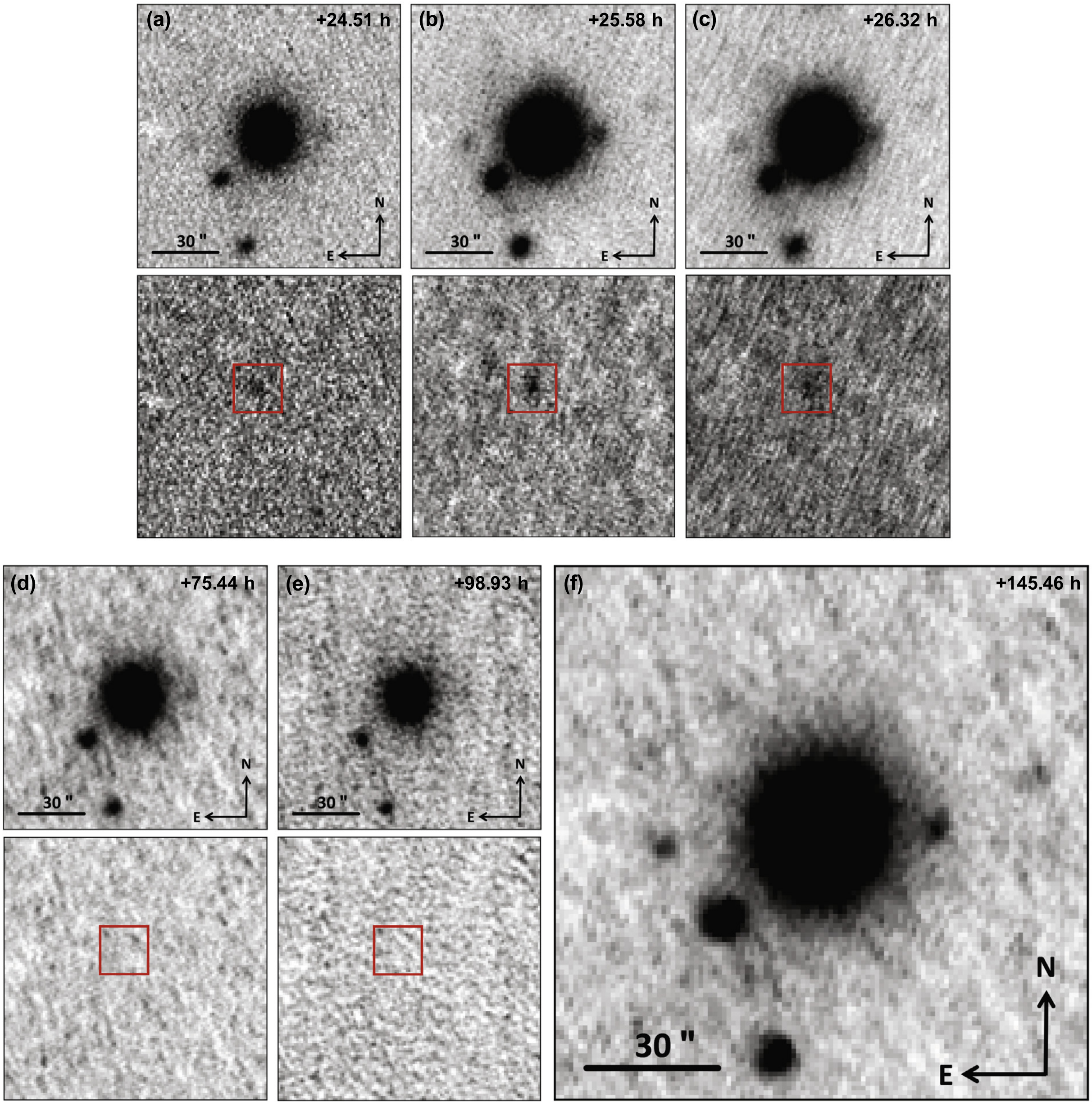

Fig. 2. (Color online) *i*-band images of NGC 4993 at 5 epochs corresponding to 24.51, 25.58, 26.32, 75.44, and 98.93 h (see Table 1) after LIGO trigger of GW 170817, shown in panel (a), (b), (c), (d), and (e) respectively. The upper rows of panels (a)–(e) show the co-added images of the galaxy NGC 4993, and the lower rows show the data with the template image subtracted. The red squares mark the position of the kilonova associated with GW170817. Panel (f) shows the template image used in the subtraction, constructed from observation on Aug 23, 2017 when the kilonova became too faint for detection by AST3-2.

For simplicity, we assume that the radiation can be approximated by a blackbody spectrum. The effective temperature of the photosphere can be written as

$$T_{\rm eff} = \left(\frac{L_{\rm MN}}{\sigma_{\rm SB} S}\right)^{1/4}, \quad (4)$$

where $\sigma_{\rm SB}$ is the Stephan–Boltzmann constant and the emitting area $S = 4\pi R_{\rm ej}^2$ with $R_{\rm ej} \simeq v_{\rm ej} t$ being the radius of the ejecta.

The redshift of the host galaxy NGC 4993 is $z = 0.009727$, which corresponds to a luminosity distance of $D_{\rm L} = 40$ Mpc adopting recent cosmological model parameters [50]. Fig. 3 shows a preliminary fit to the AST3-2 data with our analytic kilonova model. The fitting parameters are: the opacity of the ejecta $\kappa = 10\ {\rm cm^2\ g^{-1}}$, the ejecta velocity $v_{\rm ej} = 0.29c$ (c is the speed of light), and the mass of the ejecta $M_{\rm ej} = 0.0105\ M_\odot$. These numbers are consistent with typical values obtained by numerical simulations of BNS mergers [48]. Note that the opacity of the r-process ejecta with the lanthanides, $\kappa = 10 - 100\ {\rm cm^2\ g^{-1}}$, is much higher than the opacity for iron-peak elements. The above physical parameters of the ejecta for the kilonova associated with GW 170817 can be accurately determined if other multi-wavelength observations are combined with the AST3-2 data.

4. Summary

GW 170817 is the first binary neutron star merger system detected by the LIGO and Virgo detector network via gravitational wave detection. Less than a few seconds after the GW detection, a

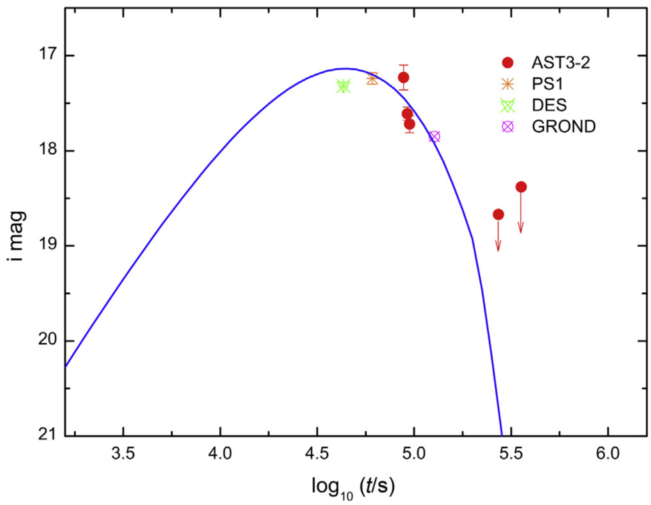

Fig. 3. (Color online) Comparison of the analytical kilonova model with AST3-2 observational data. The *X*-axis is the time in seconds after the trigger of GW 170817 by LIGO and Virgo, and the *Y*-axis is the magnitude in *i*-band. The solid red dots are the data points from AST3-2. The data points with downward arrows are 3-σ upper limits. Data points from DECam [51], PS1 [52], and GROND [53] are also shown. The blue solid line is the theoretical kilonova light curve, with $\kappa = 10$ cm^2 g^{-1}, $v_{ej} = 0.29c$, and $M_{ej} = 0.0105\ M_\odot$.

short gamma ray burst GRB 170817A, was detected by the *Fermi* and *INTEGRAL* satellites [7,8]. The optical counterpart AT2017gfo associated with GW 170817 was discovered by the 1-m Swope telescope [9] and independently by several other telescopes [10]. The host galaxy of this counterpart is NGC 4993, with a redshift of $z = 0.009727$ and corresponding distance from the Earth of $D_L = 40$ Mpc.

The AST3-2 data revealed a fast evolving transient at $t \sim 1$ day after the GW trigger, with the *i*-band magnitude fading from 17.23 ± 0.13 magnitude at $t = 24.51$ h to 17.72 ± 0.09 magnitude at $t = 26.32$ h. We also obtained two upper limits on the brightness of the optical counterpart at later times.

The brightness and temporal evolution of the detected optical transient associated with GW 170817 is in agreement with the predictions of simple kilonovae/macronovae models. Our observations support binary neutron star merger models for GW 170817. We also performed a model fit to the AST3-2 data, which leads to a preliminary estimate of the ejecta parameters. In this model, about $\sim 10^{-2}$ solar mass of radioactive material was ejected during the merger up to velocities as high as 30% the speed of light.

Conflict of interest

The authors declare that they have no conflict of interest.

Acknowledgments

The AST3 project is supported by the National Basic Research Program (973 Program) of China (2013CB834900), and the Chinese Polar Environment Comprehensive Investigation & Assessment Program (CHINARE2016-02-03), the National Natural Science Foundation of China (11573014, 11673068, 11325313, 11633002, 11433009, 11725314), and the Key Research Program of Frontier Sciences (QYZDY-SSW-SLH010, QYZDB-SSW-SYS005), the Strategic Priority Research Program "multi-waveband gravitational wave Universe" (XDB23040000) and the Youth Innovation Promotion Association (2011231) of Chinese Academy of Sciences. The construction of the AST3 telescopes was made possible by funds from Tsinghua University, Nanjing University, Beijing Normal University, University of New South Wales, Texas A&M University, the Australian Antarctic Division, and the National Collaborative Research Infrastructure Strategy (NCRIS) of Australia. It has also received funding from the Chinese Academy of Sciences through the Center for Astronomical Mega-Science and National Astronomical Observatory of China (NAOC). This research was made possible through the use of the AAVSO Photometric All-Sky Survey (APASS), funded by the Robert Martin Ayers Sciences Fund. Part of this research was funded by the Australian Research Council (ARC) Centre of Excellence for Gravitational Wave Discovery (OzGrav), CE170100004, the ARC Centre of Excellence for All-sky Astrophysics (CAASTRO), CE110001020, and the Centre of Excellence for All-sky Astrophysics in 3-Dimensions (ASTRO-3D), CE170100013. Research support to IA is provided by the Australian Astronomical Observatory (AAO). JC acknowledges the ARC Future Fellowship grant, FT130101219. Zong-Hong Zhu was supported by the National Basic Research Program (Project 973) of China (2014CB845800), the National Natural Science Foundation of China (11633001 and 11373014), and the Strategic Priority Research Program of the Chinese Academy of Sciences (XDB23000000).

References

[1] The LIGO Scientific Collaboration and the Virgo Collaboration, 2017a, GCN, 21505, 1.
[2] The LIGO Scientific Collaboration and the Virgo Collaboration, 2017b, GCN, 21509, 1.
[3] The LIGO Scientific Collaboration and the Virgo Collaboration, 2017c, GCN, 21510, 1.
[4] The LIGO Scientific Collaboration and the Virgo Collaboration, 2017d, GCN, 21513, 1.
[5] The LIGO Scientific Collaboration and the Virgo Collaboration, 2017e, GCN, 21527, 1.
[6] Abbott BP, Abbott R, Abbott TD, et al. GW170817: observation of gravitational waves from a binary neutron star inspiral. Phys Rev Lett 2017;119:161101.
[7] Connaughton V et al. GCN 2017;21506:1.
[8] Savchenko V et al. GCN 2017;21507:1.
[9] Coulter DA et al. GCN 2017;21529:1.
[10] Abbott BP, Abbott R, Adhikari RX, et al. Multi-messenger observations of a binary neutron star merger. Astrophys J Lett 2017;848:L12.
[11] Barnes J, Kasen D. Effect of a high opacity on the light curves of radioactively powered transients from compact object mergers. Astrophys J 2013;775:18.
[12] Tanaka M, Hotokezaka K, Kyutoku K, et al. Radioactively powered emission from black hole-neutron star mergers. Astrophys J 2013;780:31.
[13] Kasen D, Fernandez R, Metzger BD. Kilonova light curves from the disc wind outflows of compact object mergers. Mon Not Royal Astron Soc 2015;450:1777–86.
[14] Metzger BD, Bauswein A, Goriely S, et al. Neutron-powered precursors of kilonovae. Mon Not Royal Astron Soc 2014;446:1115–20.
[15] Barnes J, Kasen D, Wu MR, et al. Radioactivity and thermalization in the ejecta of compact object mergers and their impact on kilonova light curves. Astrophys J 2016;829:110.
[16] Li LX, Paczynski B. Transient events from neutron star mergers. Astrophys J Lett 1998;507:L59.
[17] Kulkarni SR. Modeling supernova-like explosions associated with gamma-ray bursts with short durations. arXiv preprint astro-ph/0510256, 2005.
[18] Metzger BD, Martinez-Pinedo G, Darbha S, et al. Electromagnetic counterparts of compact object mergers powered by the radioactive decay of r-process nuclei. Mon Not Royal Astron Soc 2010;406:2650–62.
[19] Kasen D, Badnell NR, Barnes J. Opacities and spectra of the r-process ejecta from neutron star mergers. Astrophys J 2013;774:25.
[20] Barnes J, Kasen D. Effect of a high opacity on the light curves of radioactively powered transients from compact object mergers. Astrophys J 2013;775:18.
[21] Tanaka M, Hotokezaka K. Radiative transfer simulations of neutron star merger ejecta. Astrophys J 2013;775:113.
[22] Barnes J, Kasen D, Wu MR, et al. Radioactivity and thermalization in the ejecta of compact object mergers and their impact on kilonova light curves. Astrophys J 2016;829:110.
[23] Metzger B. Kilonovae. Living Rev Relativ, 2017, 20:3
[24] Tanvir NR, Levan AJ, Fruchter AS, et al. A kilonova associated with short-duration gamma-ray burst 130603B. Nature 2013;500:547.
[25] Berger E, Fong W, Chornock R. An r-process kilonova associated with the short-hard GRB 130603B. Astrophys J Lett 2013;774:L23.
[26] Jin ZP, Hotokezaka K, Li X, et al. The Macronova in GRB 050709 and the GRB-macronova connection. Nat Commun 2016;7:12898.
[27] Yang B, Jin ZP, Li X, et al. A possible macronova in the late afterglow of the long-short burst GRB 060614. Nat Commun 2015;6:7323.

[28] Perley DA, Metzger BD, Granot J, et al. GRB 080503: implications of a naked short gamma-ray burst dominated by extended emission. Astrophys J 1871;2009:696.
[29] Gao H, Ding X, Wu XF, et al. GRB 080503 late afterglow re-brightening: signature of a magnetar-powered merger-nova. Astrophys J 2015;807:163.
[30] Burton MG. Astronomy Astrophys. Rev. 2010;18:417.
[31] Saunders W, Lawrence JS, Storey JWV, et al. Where is the best site on Earth? Domes A, B, C, and F, and Ridges A and B. Pub Astron Soc Pacific 2009;121:976.
[32] Wang L, Macri LM, Wang L, et al. Photometry of variable stars from Dome A, Antarctica: results from the 2010 observing season. Astronom J 2013;146:139.
[33] Wang L, Ma B, Li G, et al. Variable stars observed in the galactic disk by AST3-1 from Dome A. Antarctica. Astronom J 2017;153:104.
[34] Yang Y, Moore AM, Krisciunas K, et al. Optical sky brightness and transparency during the winter season at Dome A Antarctica from the Gattini-All-Sky Camera. Astronom J 2017;154:6.
[35] Yuan X, Su D. Optical system of the Three Antarctic Survey Telescopes. Mon Not Royal Astron Soc 2012;424:23–30.
[36] Hu Y, Shang Z, Ashley MCB, et al. Meteorological data for the astronomical site at Dome A. Antarctica. Pub Astron Soc Pacific 2014;126:868.
[37] Zhou X, Ashley MCB, Cui X, et al. Progress and results from the Chinese Small Telescope ARray (CSTAR). Astrophys Antarctica 2013;288:231.
[38] Wang L, Macri LM, Ma B, et al. Stellar variability from Dome A, Antarctica. EPJ Web of Conferences. EDP Sciences 2017;152:02010.
[39] Hu L et al. GCN 2017;21883:1.
[40] Van Dokkum PG. Cosmic-ray rejection by Laplacian edge detection. Pub Astron Soc Pacific 2001;113:1420.
[41] Freyhammer LM, Andersen MI, Arentoft T, et al. On cross-talk correction of images from multiple-port CCDs. Exp Astro 2001;12:147–62.
[42] Bertin E, Mellier Y, Radovich M, et al. The terapix pipeline. Astron Data Analy Soft Syst XI 2002;281:228.
[43] Annis J, Soares-Santos M, Strauss MA, et al. The sloan digital sky survey coadd: 275 deg2 of deep sloan digital sky survey imaging on stripe 82. Astrophys J 2014;794:120.
[44] Miller JP, Pennypacker CR, White GL. Optimal image subtraction method: summary derivations, applications, and publicly shared application using IDL. Pub Astron Soc Pacific 2008;120:449.
[45] Henden AA, Levine SE, Terrell D, et al. Data Release 3 of the AAVSO All-Sky Photometric Survey (APASS). J Am Assoc Variable Star Observers (JAAVSO) 2012;40:430.
[46] Faherty JK, Tinney CG, Skemer A, et al. Indications of water clouds in the coldest known brown dwarf. Astrophys J Lett 2014;793:L16.
[47] Kawaguchi K, Kyutoku K, Shibata M, et al. Models of Kilonova/Macronova emission from black holeCneutron star mergers. Astrophys J 2016;825:52.
[48] Dietrich T, Ujevic M. Modeling dynamical ejecta from binary neutron star mergers and implications for electromagnetic counterparts. Class Quan Gravity 2017;34:105014.
[49] Xiao D, Liu LD, Dai ZG, et al. Afterglows and macronovae associated with nearby low-luminosity short-duration gamma-ray bursts. arXiv:1710.00275, 2017.
[50] Freedman WL, Madore BF, Gibson BK, et al. Final results from the Hubble Space Telescope key project to measure the Hubble constant. Astrophys J 2001;553:47.
[51] Allam S et al. GCN 2017;21530:1.
[52] Chambers KC et al. GCN 2017;21553:1.
[53] Smartt SJ, Chen TW, Jerkstrand A, et al. A kilonova as the electromagnetic counterpart to a gravitational-wave source. Astrophys J 2017:47. arXiv:1710.05841.